Supporting Information

Biogeochemical Changes and Mercury Methylation beneath an In-Situ Sediment Cap

Nathan W. Johnson, Danny D. Reible, Lynn E. Katz*

University of Texas at Austin, Department of Civil Architectural and Environmental Engineering

*Corresponding author, Phone: (512)471-4642, Fax: 471-5870, reible@mail.utexas.edu

17 pages; 10 tables, 5 figures, 7 equations

BROOKS RAND MEHG LABORATORY QA/QC RESULTS

Ongoing precision and recovery results fell within standard operating procedures as defined by EPA Method 1630. Although small sample mass was used (<2g), the concentration in all samples (except for capping material) was above the method reporting limit adjusted for the use of lower sample mass (MRL 0.034-0.117 ng/g). QA/QC results reported herein are only for analytical analyses with samples from the present study. Recovery of reference material (CC-580) averaged 87% during the analysis of our samples (n=3). The RPD of duplicate analyses of our samples averaged 11% (n=3). MS/MSD recovery averaged 108% (n=6) and RPD for MS/MSD averaged 16% (n=3).

MICROCOSM SCHEMATIC

The acrylic sediment microcosms used in this study have a bottom section to hold sediment that measures 15x5x7cm. The water column is supported by a 3cm weir and measures 25x5x6cm.

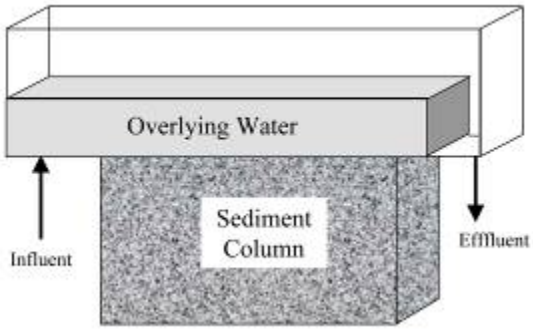

Figure S1 Schematic of experimental microcosms. 7.5cm sediment depth with 3cm overlying water.

TOTAL MERCURY CONCENTRATIONS

Little variability in total mercury concentration was observed in both uncapped and capped microcosms suggesting that the observed differences in methylmercury concentration (Figure 2) were due to differences in methylmercury production rather than differences in total mercury concentrations.

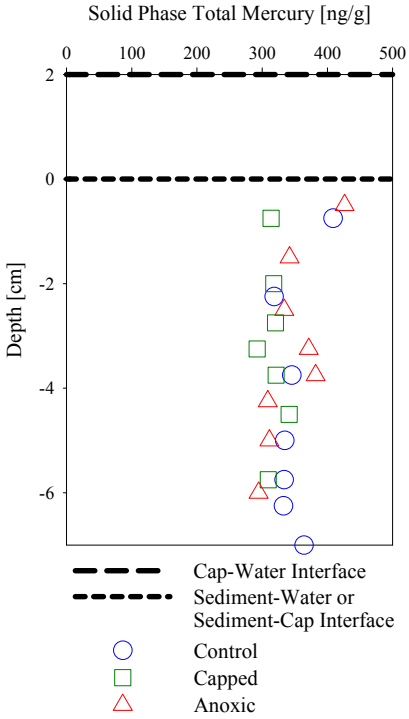

Figure S2 Total mercury concentrations in control and capped microcosms

IRON OXIDATION RATE SENSITIVITY SIMULATIONS

A sensitivity analysis of iron oxidation rates that resulted in the oxidation of 5, 10, and 15umol/cm2 ferric iron (kFeOX= 4.8x105, 1.6x106, and 1.6x107 uM-1year-1, respectively) during the initial 22 day period in which all sediments were exposed to oxic water is shown in Figure S3 (a-c for control, d-f for capped, g-i for anoxic). Model predictions (120 days) show a range in the depth of the onset of sulfate reduction. This range of transition to sulfate reduction is more sensitive to the initial mass of oxidized iron in the anoxic system (0.5cm – 4.5cm range) than in the control (5.5cm – 6.5cm) or capped (3cm – 5cm) system (Figure 2).

The lower methylmercury at 0-2cm depth in the capped treatment coincides with an area where dissolved ferrous iron was present and visual observations showed that the surficial sediment beneath the cap was not as reduced as the surficial sediment in the anoxic treatment. Ferrous iron produced near the surface of the anoxic treatment could have diffused out into the overlying water and been oxidized at the surface or carried away. In the capped treatment, however, a broader oxic zone within the cap may have re-oxidized ferrous iron and prevented its loss to the overlying water. The ferrous/ferric iron cycling in the surficial sediment underlying the sediment cap may have prevented maximum methylmercury production at 0-2cm below the cap-sediment interface, and is a result that highlights the need to consider the geochemical effects of capping in detail during cap design and monitoring.

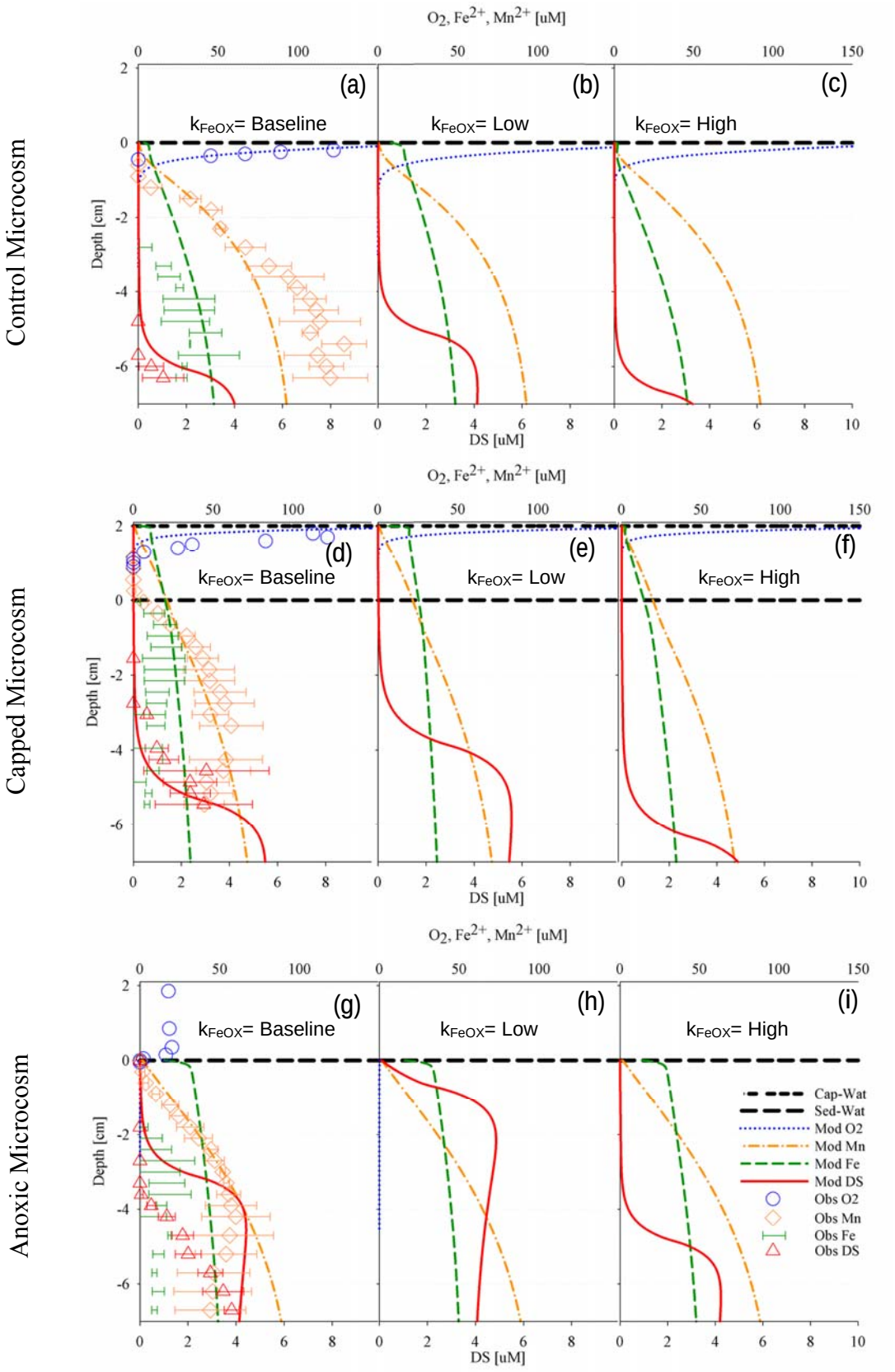
Control Microcosm
Capped Microcosm
Anoxic Microcosm
O2, Fe2+, Mn2+ [uM]
Depth [cm]
DS [uM]
(a)
(b)
(c)
(d)
(e)
(f)
(g)
(h)
(i)
kFeOX= Baseline
kFeOX= Low
kFeOX= High
Cap-Wat
Sed-Wat
Mod O2
Mod Mn
Mod Fe
Mod DS
Obs O2
Obs Mn
Obs Fe
Obs DS

Figure S3. Sensitivity analysis of model predictions to initial oxidized iron in the surficial sediment. (a) – Baseline, 10umol/cm^2 initial iron oxidized, k_{FeOX}=1.6(10^6) $\mu M^{-1}yr^{-1}$) and sensitivity analysis of iron oxidation rates (b) – Low rate, 5umol/cm^2 or k_{FeOX}=4.8(10^5) $\mu M^{-1}yr^{-1}$, and (c) – High rate 15umol/cm^2 or k_{FeOX}=1.6(10^7) $\mu M^{-1}yr^{-1}$) for control microcosm. Model predictions for capped and anoxic microcosms at 120 days are shown in (d) and (g) respectively, with associated iron oxidation sensitivity analysis in (e,f) and (h,i) respectively.

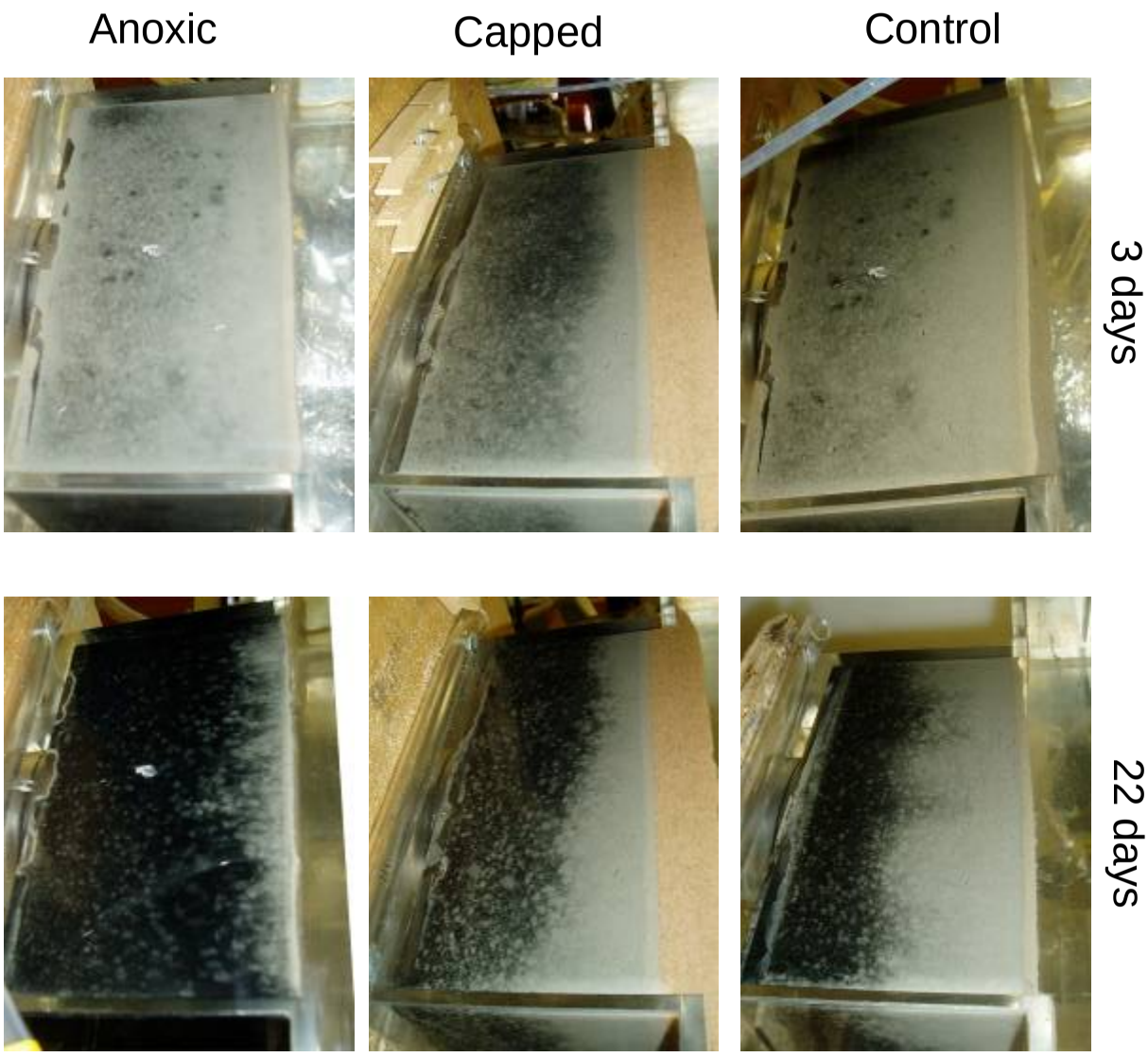

Figure S4 Visual observations of differences amongst sediment treatments at 3 and 22 days after cap placement

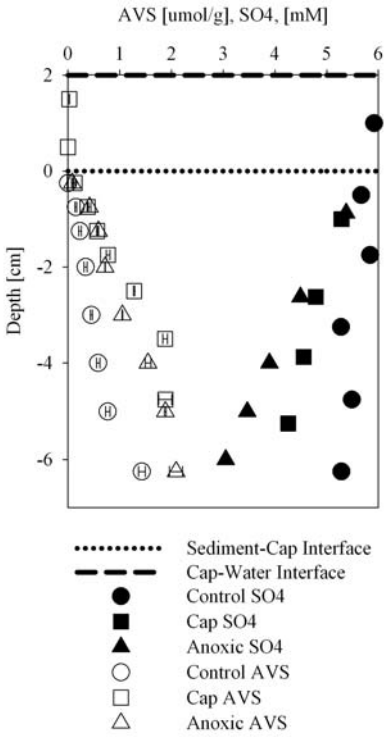

Figure S5 Depth profiles of SO_4^{2-} and AVS concentrations in control, capped and anoxic microcosms at the close of experiments

Evidence of increased sulfate reduction at shallower depths in capped and anoxic microcosms was observed in solid-phase AVS and porewater sulfate concentrations. Figure S5 shows results from cores taken at 125 days. Error bars on AVS measurements lie within the open symbols, however, limited sample volume allowed only one SO_4^{2-} measurement to be obtained at each depth. In the control microcosm (circles), AVS remains low (<1μmol/g) at depths less than 6cm, and little sulfate depletion is observed. However, in both capped (squares) and anoxic (triangles) microcosms, AVS and SO_4^{2-} observations are consistent with increased sulfate reduction at depths between 2-5cm. On a mole per volume basis, the increase in AVS in the capped and anoxic microcosms was greater than the reduction in sulfate (1.8 vs. 0.8μmol/cm^3_T; using bulk density of 1.2g/cm^3, porosity of 0.5). The continued diffusion of sulfate into the sediment, driven by the observed concentration gradient, followed by biological reduction and precipitation to immobile metal sulfides leads to a buildup of solid-phase sulfides in saltwater sediments. Iron concentrations observed at ~20-100μM in all microcosms are sufficient to promote iron-sulfide precipitate formation in the presence of dissolved sulfide at pH 7-8 ($Fe^{2+}+HS^-=FeS_{(s)}+H^+$; $logK_{sp}$=-4.2 *(28)*). The depletion of AVS near the sediment surface in all microcosms, including the capped/anoxic microcosms, is likely due to the oxidation of metal sulfides by oxygen during the initial 3 weeks of oxic overlying water conditions before the initiation of capped/anoxic conditions.

MODEL FORMULATION

The constitutive equations for dissolved and solid constituents, as outlined by Boudreau are presented below. Specific model reactions, stoichiometry, and rates are presented in Table S1. Initial and boundary conditions as well and other model parameters are presented in Tables S2-4.

First order finite difference schemes for uneven grid spacing were substituted for all spatial derivatives. The Method of Lines was used to solve the resulting set of ordinary differential equations as an initial value problem.

$$\varphi\frac{\partial C}{\partial t} = D\frac{\partial}{\partial x}\left(\frac{\varphi}{\theta^2}\frac{\partial C}{\partial x}\right) - \frac{\partial(\varphi u C)}{\partial x} + Rxn$$

$$\theta^2 = \varphi^{-p}$$

$$\frac{\partial C}{\partial t} = \frac{1}{\varphi}\left[D\frac{\partial}{\partial x}\left(\varphi^{p+1}\frac{\partial C}{\partial x}\right) - \frac{\partial(\varphi u C)}{\partial x} + Rxn\right]$$

$$\frac{\partial C}{\partial t} = \frac{D}{\varphi}\left[\varphi^{p+1}\frac{\partial^2 C}{\partial x^2} + (p+1)\varphi^p\frac{\partial\varphi}{\partial x}\bigg|_x\frac{\partial C}{\partial x}\right] - \frac{1}{\varphi}\left(\varphi u\frac{\partial C}{\partial x} + \varphi\frac{\partial u}{\partial x}\bigg|_x C + \frac{\partial\varphi}{\partial x}\bigg|_x uC\right) + \frac{1}{\varphi}(+Rxn)$$

$$\frac{\partial C}{\partial t} = \frac{D}{\varphi}\left[\varphi^{p+1}\frac{\partial^2 C}{\partial x^2} + \left((p+1)\varphi^p\frac{\partial\varphi}{\partial x}\bigg|_x\right)\frac{\partial C}{\partial x}\right] - \left[u\frac{\partial C}{\partial x} + C\left(\frac{u}{\varphi}\frac{\partial\varphi}{\partial x}\bigg|_x + \frac{\partial u}{\partial x}\bigg|_x\right)\right] + \frac{1}{\varphi}(+Rxn)$$

where:

- φ = function of depth, calibrated to observations
- p = 2.0
- u = 0.0 [cm/day]
- D = molecular diffusivity of species [cm^2/day]
- Rxn = as defined below [umol/cm^3/day

For solid-phase constituents:

$$\varphi_s\frac{\partial B}{\partial t} = \frac{\partial}{\partial x}\left(\varphi_s D_B\frac{\partial B}{\partial x}\right) - \frac{\partial(\varphi_s wB)}{\partial x} + \varphi_s Rxn$$

$$\frac{\partial B}{\partial t} = \frac{1}{\varphi_s}\left[\frac{\partial}{\partial x}\left(\varphi_s D_B\frac{\partial B}{\partial x}\right) - \frac{\partial(\varphi_s wB)}{\partial x} + \varphi_s Rxn\right]$$

$$\frac{\partial B}{\partial t} = \frac{1}{\varphi_s}\left[\begin{array}{l}\varphi_s D_B\frac{\partial^2 B}{\partial x^2} + \varphi_s\frac{\partial D_B}{\partial x}\bigg|_x\frac{\partial B}{\partial x} + \frac{\partial\varphi_s}{\partial x}\bigg|_x D_B\frac{\partial B}{\partial x} \\ \qquad -\left(\varphi_s w\frac{\partial B}{\partial x} + \varphi_s\frac{\partial w}{\partial x}\bigg|_x B + \frac{\partial\varphi_s}{\partial x}\bigg|_x wB\right) + \varphi_s Rxn\end{array}\right]$$

$$\frac{\partial B}{\partial t} = D_B\frac{\partial^2 B}{\partial x^2} + \left(\frac{\partial D_B}{\partial x}\bigg|_x + \frac{D_B}{\varphi_s}\frac{\partial\varphi_s}{\partial x}\bigg|_x\right)\frac{\partial B}{\partial x} - \left[w\frac{\partial B}{\partial x} + \left(\frac{w}{\varphi_s}\frac{\partial\varphi_s}{\partial x}\bigg|_x + \frac{\partial w}{\partial x}\bigg|_x\right)B\right] + Rxn$$

where:

- φ_s is 1-φ [g/cm^3]
- w, the particle burial velocity, was set to 0.0 [cm/day]
- D_B was set to 7.5x10^{-8} [cm^2/day]

REACTIONS

Reactions (the term "Rxn") is defined on a total volume basis μmol/cm^3_T/day for solid and mmol/L_T/day for liquid. In the actual code, the RHS of the mass balance for each constituent is divided through by either ψ [L_{water}/L_{total}] or ψ_s[g_{sed}/cm^3_{tot}] and care was taken in defining the units of reaction terms. Representative equations used for each type of reaction (Table S1) are shown below.

PO – Primary Oxidation of organic matter

SO – Secondary oxidation/reduction reactions

PREC – precipitation of metal-sulfides

SORB – sorption of metals to solid phase

$$Rxn = R_{PO} + R_{SO} + R_{PREC} + R_{SORB}$$

$$R_{PO}\Big|_{O2}\left[\frac{mmol}{L_T - day}\right] = kmax_{O2}\left[\frac{mmol}{L_T - day}\right]\left(\frac{C_{O2}}{KI_{O2} + C_{O2}}\right)\left(\frac{C_{POC}}{KI_{POC} + C_{POC}}\right)$$

$$R_{SO}\Big|_{FeS-O2}\left[\frac{mmol}{L_T - day}\right] = k_{FeS-O2}\left[\frac{L_T}{mmol - day}\right]C_{O2}\varphi\left[\frac{mmol}{L_T}\right]C_{FeS}\varphi_s\left[\frac{umol}{cm^3{}_T}\right]$$

$$R_{PREC}\Big|_{Fe-S}\left[\frac{mmol}{L_T - day}\right] = k_{prec-FeS}\left[\frac{mmol}{L_T - day}\right](\Omega_{FeS} - 1) : \Omega_{FeS} = \frac{Fe^{2+}\left[\frac{mmol}{L_w}\right]DS\left[\frac{mmol}{L_w}\right]}{H^+\left[\frac{mmol}{L_w}\right]K_{sp}\left[\frac{mmol}{L_w}\right]}$$

$$R_{SORB}\Big|_{Fe2}\left[\frac{mmol}{L_T - day}\right] = k_{ads-Fe}\left[\frac{L_w}{g_s - day}\right]\varphi_s\left[\frac{g_s}{cm^3{}_T}\right]\left[\frac{1000cm^3{}_T}{L_T}\right]\left(C_{Mn2}\left[\frac{mmol}{L_w}\right] - \frac{C_{Mn2s}\left[\frac{umol}{g_s}\right]\left[\frac{1mmol}{1000umol}\right]}{K_D\left[\frac{L_w}{kg_s}\right]\left[\frac{1kg_s}{1000g_s}\right]}\right)$$

Table S1
Reactions and constituents included in modeling

DESCRIPTION	STOICHIOMETRY	RATE	UNITS	SOURCE
Primary Reactions (biological organic matter degradation)				
Aerobic Respiration	O_2 + POC[a] = DIC[a]	200,100,0.5[b]	uM/day,uM,uM	Calibrated
Nitrate Reduction	NO_3 +POC = DIC	30, 20, 6	uM/day,uM,uM	Calibrated
Manganese Reduction	Mn^{4+} + POC = DIC + Mn^{2+}	0.2, 1, 0.001	uM/day, umol/g	Ref. 27
Iron Reduction	Fe^{4+} + POC = DIC + Fe^{2+}	0.032, 1, 0.005	uM/day, umol/g	Ref. 27
Sulfate Reduction	SO_4^{2-} + POC = DIC + HS^-	18, 10, 15	uM/day,uM,uM	Calibrated
Methanogenesis	POC = DIC + CH_4^+	0.05, N/A, N/A	uM/day,-,-	
POC		N/A, 0.1, N/A	-,umol/g,-	
Secondary Oxidation/Reduction Reactions				
By O_2				
Mn^{2+}	Mn^{4+} + 0.5O_2 = Mn^{2+}	4.6	$(mol/L)^{-1}yr^{-1}$	Ref. 27
Fe^{2+}	Fe^{4+} + 0.25O_2 = Fe^{2+}	$1.6x10^6$	$(mol/L)^{-1}yr^{-1}$	Sensitivity Analysis
HS^-	SO_4^{2-} + 2O_2 = HS^-	$2.0x10^5$	$(mol/L)^{-1}yr^{-1}$	Ref. 27
CH_4^+	CH_4^+ + 2O_2 = DIC	$1.0x10^{10}$	$(mol/L)^{-1}yr^{-1}$	
$MnS_{(s)}$	$MnS_{(s)}$ + 2O_2 = Mn^{2+} + HS^-	$3.0x10^5$	$(mol/L)^{-1}yr^{-1}$	
$FeS_{(s)}$	$FeS_{(s)}$ + 2O_2 = Fe^{2+} + HS^-	$3.0x10^5$	$(mol/L)^{-1}yr^{-1}$	Ref. 27
R-$Mn^{2+}{}_{(s)}$[a]	R-$Mn^{2+}{}_{(s)}$ + O_2 = Mn^{2+}	$2.1x10^7$	$(mol/L)^{-1}yr^{-1}$	Ref. 27
R-$Fe^{2+}{}_{(s)}$[a]	R-$Fe^{2+}{}_{(s)}$ + O_2 = Fe^{2+}	$1.6x10^8$	$(mol/L)^{-1}yr^{-1}$	Ref. 27
By Mn^{2+}				
Fe^{2+}	0.5Mn^{4+} + Fe^{2+} = 0.5Mn^{2+} + Fe^{3+}	$1.0x10^4$	$(mol/L)^{-1}yr^{-1}$	Ref. 27
HS^-	4Mn^{4+} + HS^- = 4Mn^{2+} + SO_4^{2-}	$8.0x10^5$	$(mol/L)^{-1}yr^{-1}$	Ref. 27
By Fe^{2+}				
HS^-	Fe^{4+} + HS^- = Fe^{2+} + SO_4^{2-}	$1.0x10^3$	$(mol/L)^{-1}yr^{-1}$	Ref. 27
Precipitation/Dissolution				
Manganese-Sulfide	Mn^{2+} + HS^- = $MnS_{(s)}$ + H^+	$10^{3.1}$, 0.1[c]	mol/L, umol/g/yr	Ref. 22, Calibrated
Iron-Sulfide	Fe^{2+} + HS^- = $FeS_{(s)}$ + H^+	$10^{-4.2}$, 0.1[c]	mol/L, umol/g/yr	Ref. 22, Calibrated
Solid-phase Sorption				
Manganese sorption	Mn^{2+} = R-$Mn^{2+}{}_{(s)}$	3.0, 150[d]	L/kg, L/g/day	Calibrated
Iron sorption	Fe^{2+} = R-$Fe^{2+}{}_{(s)}$	800, 150[d]	L/kg, L/g/day	Calibrated

[a] abbreviations: POC–Particulate Organic Carbon; DIC–Dissolved Inorganic Carbon; 'R-'–Organo & solid oxide -metal complexes
[b] Maximum utilization rate[uM/day], Half saturation constant [uM or umol/g], Threshold concentration [uM or umol/g], respectively
[c] K_{sp} [mol/L], Precipitation rate [umol/g/year]K_d [L/kg], Adsorption rate [L/g/day]
[d] K_d [L/kg], Adsorption rate [L/g/day]

Table S2 Initial Conditions

Primary Constituents	Control	Anoxic	Cap	Comment
POC	250 µmol/g	250	2.5	75% of meas. OC
O_2	0.000 mM	0.000	0.0	
NO_3	0.000 mM	0.000	0.0	
Mn^{4+}	0.000 µmol/g	0.000	0.0	All reduced initially
Fe^{3+}	0.00 µmol/g	0.000	0.0	All reduced initially
SO_4^{2-}	1.0 mM	1.0	1.0	~80% reduced
HCO_3^-	0.46 mM	0.46	0.46	
Mn^{2+}	0.178 mM	0.158	0	~Equil. w/solid
Fe^{2+}	0.059 mM	0.059	0	~Equil. w/solid
HS^-	0.0 mM	0.0	0	
CH_4	0.0 mM	0.0	0	
$MnS_{(s)}$	0.038 µmol/g	0.038	0	5% of total metal
$FeS_{(s)}$	2.5 µmol/g	2.5	0	5% of total metal
R-Mn^{2+}	0.534 µmol/g	0.564	0.75	All reduced initially
R-Fe^{2+}	47.44 µmol/g	47.44	50.0	All reduced initially

Table S3 Boundary Conditions

Primary Constituents	Control	Anoxic	Cap	Comments
O_2	0.26 mM	0.0026	0.26	Saturated
NO_3	0.1 mM	0.1	0.1	25% of 5mg/L
Mn^{4+}	0.0 (Flux)	0.0	0.0	
Fe^{3+}	0.0 (Flux)	0.0	0.0	
SO_4^{2-}	6.0 mM	6.0	6.0	25% of 24mM, observe
HCO_3^-	0.46 mM	0.46	0.46	
Mn^{2+}	0.0 mM	0.0	0.0	
Fe^{2+}	0.0 mM	0.0	0.0	
HS^-	0.0 mM	0.0	0.0	
CH_4	0.0 mM	0.0	0.0	
$FeS_{(s)}$	0 (Flux)	0.0	0.0	
TOTH	$1.65E^{-5}$	$1.65E^{-5}$	$1.65E^{-5}$	
R-Mn^{2+}	0.0 (Flux)	0.0	0.0	
R-Fe^{2+}	0.0 (Flux)	0.0	0.0	

Table S4 Other Parameters

	Control	Anoxic	Cap
Particle diffusion	2.36cm^2/year	2.36 (7.5E-8 cm2/sec)	2.36
Domain length	7.0 cm	7.0 cm	7.0cm+2cm cap = 9cm total
Porosity	f(depth)	f(depth)	0.35
Diffusive boundary	0.2 cm	0.2 cm	0.2 cm

REPRESENTATIVE POREWATER DATA

Tables S5-7 present representative geochemical data from 120 day observations. Depth for oxygen measurements is presented separately from depth for Mn(II), Fe(II), and DS. Averages and standard deviations are reported for Mn(II) and DS at each depth are based on measurements from 3 independently calibrated electrodes. The value for each electrode at each depth represents the average of triplicate scans at that depth. A range of values (high and low) is reported for Fe(II) based on duplicate electrode measurements.

Table S5 Measurements of O_2, Mn(II), Fe(II), and DS in Control microcosm at 120 days.

Control Microcosm								
O2			Mn(II)		Fe(II)		DS	
Depth	Average	Depth	Average	Stdev (n=3)	High	Low	Average	Stdev (n=3)
1.15	276.5	0			0.00	0.00		
0.65	265.5	-0.3			0.00	0.00		
0.45	265.5	-0.6	0.00	0.00	0.00	0.00		
0.25	265.5	-0.9	0.00	0.00	0.00	0.00		0.00
0.15	260	-1.2	7.88	6.96	0.00	0.00		0.00
0.1	254.4	-1.5	32.66	6.73	0.00	0.00		
0.05	248.9	-1.8	45.51	7.01	0.00	0.00		0.00
0	235.1	-2.3	51.49	3.16	0.00	0.00		0.00
-0.05	213.5	-2.8	67.11	12.74	8.61	0.00		
-0.1	189.7	-3.3	81.83	14.18	20.62	11.04		0.00
-0.15	158.2	-3.6	93.85	22.50	26.25	12.26		0.00
-0.2	122.2	-3.9	99.38	5.85	23.53	28.25		
-0.25	89.0	-4.2	107.50	10.17	47.97	15.63		0.00
-0.3	66.9	-4.5	111.48	13.83	47.82	16.20		0.00
-0.35	45.3	-4.8	113.73	25.42	44.70	14.45	0.00	0.00
-0.45	0	-5.1	107.65	5.09	52.26	31.93		0.00
		-5.4	128.92	14.07	32.02	32.72		0.00
		-5.7	112.15	20.80	25.20	63.31	0.00	0.00
		-6	117.83	10.74	27.46	30.50	0.54	0.51
		-6.3	120.27	23.39	23.65	30.65	1.04	0.86

Table S6 Measurements of O_2, Mn(II), Fe(II), and DS in Capped microcosm at 120 days.

Capped Microcosm								
O2			Mn(II)		Fe(II)		DS	
Depth	Average	Depth	Average	Stdev (n=3)	High	Low	Average	Stdev (n=3)
3.20	260.0	1.95						
2.70	260.0	1.45						
2.50	260.0	1.15	0.00	0.00	0.00	0.00		
2.30	260.0	0.85	0.00	0.00	0.00	0.00		
2.10	239.4	0.55	0.00	0.00	0.00	0.00		
1.90	176.6	0.25	0.58	1.01	0.00	0.00		
1.80	112.5	-0.05	6.48	2.56	0.00	4.69		
1.70	121.5	-0.35	15.31	2.64	19.62	6.51		
1.60	82.8	-0.65	23.23	2.61	27.03	12.62		
1.50	36.9	-0.95	33.44	5.11	28.12	8.63		
1.40	27.8	-1.25	39.05	9.13	30.41	10.96		
1.30	6.7	-1.55	43.49	9.68	32.37	5.75		
1.20	0.0	-1.85	47.39	15.86	32.70	6.92	0.00	0.00
1.10	0.0	-2.15	47.83	15.55	32.05	6.92		
1.00	0.0	-2.45	54.25	16.29	22.45	7.69		
0.90	0.0	-2.75	57.13	18.57	20.93	8.19		
		-3.05	48.20	11.43	20.06	0.00	0.00	0.00
		-3.35	61.27	19.89	19.84	8.30	0.56	0.11
		-3.65	39.51	4.70	18.09	0.00		
		-3.95	58.02	22.90	18.31	18.26	0.98	0.48
		-4.25	56.34	17.08	8.502	16.04	1.26	
		-4.55	45.80	14.13	7.957	0	3.03	2.60
		-4.85	48.53	14.03	7.303	11.73	2.36	1.11
		-5.15	44.40	12.47	6.867	10.40	2.36	0.837
		-5.45	38.51	10.89	6.104	8.632	2.92	2.02

Table S7 Measurements of O_2, Mn(II), Fe(II), and DS in Anoxic microcosm at 120 days.

Anoxic Microcosm								
O2			Mn(II)		Fe(II)		DS	
Depth	Average	Depth	Average	Stdev (n=3)	High	Low	Average	Stdev (n=3)
3.35	19.0	0	0.00	0.00	0.00	0.00	0.00	0.00
2.85	20.0	-0.3	1.64	1.46	0.00	0.00		
2.35	20.0	-0.6	3.63	1.70	0.00	0.00		
1.85	17.9	-0.9	9.97	2.38	0.00	0.00		
0.85	18.4	-1.2	19.05	5.34	0.00	0.00		
0.35	20.0	-1.5	24.29	5.72	0.00	0.00		
0.15	16.3	-1.8	31.45	8.59	5.09	0.00	0.00	0.00
0.05	2.2	-2.1	36.71	8.81	13.93	0.00		
0.00	0.0	-2.4	44.37	4.54	19.76	0.00		
-0.05	0.0	-2.7	46.88	5.97	34.35	0.00	0.00	0.00
		-3	51.86	1.78	25.10	0.00		
		-3.3	54.17	1.84	28.07	5.67	0.00	0.00
		-3.6	55.56	7.41	32.04	5.48	0.05	0.09
		-3.9	57.08	16.06	16.80	10.46	0.47	0.18
		-4.2	60.07	21.47	16.72	0.00	1.12	0.35
		-4.7	56.27	27.44	19.38	17.47	1.78	0.44
		-5.2	54.00	19.35	8.04	15.20	2.01	0.54
		-5.7	46.16	22.69	7.59	10.66	2.93	0.52
		-6.2	45.65	24.30	7.76	15.26	3.47	0.85
		-6.7	44.13	22.16	7.34	10.88	3.82	0.31

METHYL MERCURY OBSERVATIONS

Tables S8-10 present methylmercury observations [pg/g-dry] made at 120 days after cap placement, total mercury concentrations in split, homogenized samples [ng/g-dry], and % MeHg.

Table S8 MeHg in Control Microcosm at 120 days

Control Microcosm			
Depth	MeHg [pg/gdry]	Total Hg [ng/g]	% MeHg
0.75	154	409	0.038
2.25	154	318	0.048
3.75	171	345	0.049
5	220	335	0.066
5.75	209	334	0.063
6.25	180	333	0.054
7	219	364	0.060

Table S9 MeHg in Capped microcosm at 120 days

Capped Microcosm			
Depth	MeHg [pg/gdry]	Total Hg [ng/g]	% MeHg
-1.5	19	40	
-0.5	20	1	
0.75	149	314	0.047
2	188	318	0.059
2.75	255	320	0.080
3.25	271	292	0.093
3.75	241	321	0.075
4.5	235	341	0.069
5.75	215	309	0.069

Table S10 MeHg in Anoxic microcosm at 120 days

Anoxic Microcosm			
Depth	MHg [pg/gdry]	Total Hg [ng/g]	% MHg
0.5	213	426	0.050
1.5	258	342	0.075
2.5	222	334	0.066
3.25	270	372	0.073
3.75	223	382	0.058
4.25	161	309	0.052
5	262	311	0.084
6	232	295	0.079

An estimate for the uncertainty in methylmercury concentrations was made using the pooled variance of replicate analytical analyses. The estimated standard deviation was 22.5pg/g and was used to calculate the significance of differences between the control and capped treatment in the area of transition to sulfate reduction in the capped and anoxic microcosm. For the capped microcosm, average values between 2.25 and 5cm depth were compared using a separate variance, two-tailed T-test. The p value for the

difference in the average methylmercury between capped (n=4) and control (n=3) treatments in this zone of transition to sulfate reduction was p=0.0018. The p value for the difference in the average methylmercury between anoxic (n=7) and control (n=3) treatments in the zone of transition to sulfate reduction (0.5 to 5cm) was p=0.0058.